

Changes of soil thermal and hydraulic regimes in the Heihe River Basin

Xiaoqing Peng · Cuicui Mu

Received: 30 November 2016 / Accepted: 16 August 2017 / Published online: 2 September 2017
© Springer International Publishing AG 2017

Abstract Soil thermal and hydraulic regimes are critical factors influencing terrestrial processes in cold regions. Collection of field data from frozen ground has occurred at point scales, but limited data exist that characterize changes of soil thermal and hydraulic regimes at the scale of the whole Heihe River Basin. This study uses a long-term regional climate model coupled with land surface model to investigate the soil thermal and hydraulic regime changes at a large spatial scale. It also explores potential factors, including the climate and non-climate factors. Results show that there is significant variability in mean annual air temperature (MAAT) of about 0.47 °C/decade during 1980–2013. A time series of area-averaged mean annual soil temperature (MAST) over the whole Heihe River Basin shows a significant increase between 0.25 and 0.36 °C/decade during 1984–2013, with a net change of 0.9 °C. A trend of increasing wetness is found in soil moisture. Frozen days (FD) decreased significantly both in seasonally frozen ground (SFG) regions and permafrost regions, with a net change between 7 and 13 days during 1984–2013. Freezing index (FI) had a positive effect on FD, while thawing index (TI), MAAT, precipitation, and normalized difference vegetation index (NDVI) had a negative effect. These results are important to understand dynamic mechanisms of soil freeze/thaw cycles.

Keywords Soil temperature · Soil moisture · Heihe River Basin

Introduction

Recently, climate change and extreme weather events have drawn great public attention. General circulation model (GCM) results indicate that global warming will continue, and its amplitude will increase during the twenty-first century. The Fifth Assessment Report (AR5) of the Intergovernmental Panel on Climate Change (IPCC) has demonstrated that the global mean temperature has warmed by 0.85 °C from 1880 to 2012 (IPCC 2013). The rates and magnitude of temperature rise were much greater at high latitudes (Serreze et al. 2000; Hinzman et al. 2005; Screen and Simmonds 2010; Jeong et al. 2012) and in high altitudes (Pepin et al. 2015; Guo and Wang 2016) when compared to the global mean temperature. Hence, researches at high latitudes and high altitudes are needed to understand this difference.

Climate warming has resulted in worldwide permafrost degradation and seasonally frozen ground (SFG) changes, including an increase in active layer thickness (Zhang et al. 2005; Zhao et al. 2010; Kaverin et al. 2012; Shiklomanov 2012; Luo et al. 2016; Park et al. 2016; Wu et al. 2016), a decrease in the areal extent of permafrost (Koven et al. 2013; Slater and Lawrence 2013; Guo and Wang 2016), and decrease in soil frozen depth in SFG (Frauenfeld and Zhang 2011; Peng et al. 2016). These changes can subsequently also affect geomorphic

X. Peng · C. Mu (✉)
Key Laboratory of Western China's Environmental Systems
(Ministry of Education), College of Earth and Environmental
Sciences, Lanzhou University, Lanzhou 730000, China
e-mail: muc@lzu.edu.cn

processes, hydrologic processes (Ford and Frauenfeld 2016), ecosystem processes (Yi et al. 2011), and infrastructure in cold regions (Gruber et al. 2004). There is a large amount of carbon storage in permafrost regions. Rising air temperature can affect permafrost thawing, resulting in further carbon release into the atmosphere that would accelerate climate warming (Mu et al. 2015; Schuur et al. 2015; Schädel et al. 2016).

Soil thermal and hydraulic regimes play an important role in cold regions. Specifically, permafrost and SFG changes can alter soil thermal and hydraulic regimes that are prominent in the freeze-thaw process. Almost all ecological, hydrological, pedological, and biological activities occur within, or interact with, soil thermal and hydraulic regimes (Hinzman et al. 1991; Kane et al. 1991). Soil thermal and hydraulic regime variability may influence ecosystem carbon and nutrient losses (Henry 2008). At the same time, microbial cells, soil aggregates, plant material, particulate and soluble material, trace gas losses and other associated materials all play roles and exert influences on this process (DeLuca et al. 1992; Melick and Seppelt 1992; Wang and Bettany 1993; Vaz et al. 1994; Chen et al. 1995; Harris and Safford 1996; Skogland et al. 1988; Chang and Hao 2001; Larsen et al. 2002; Müller et al. 2002; Oztas and Fayetorbay 2003; Six et al. 2004; Yanai et al. 2004).

Soil thermal and hydraulic regimes also affect heat exchange between atmosphere and land surface (Zhao et al. 2004). From late fall to early spring, a time when plants are largely inactive, rising temperature potentially affects ecosystem carbon and nutrient cycling by altering the soil thermal and hydraulic regimes (Henry 2008). It also has a significant impact on the surface energy and moisture balance. The thermal conductivity differences between frozen and thawing soil result in significant differences in soil heat flux. During the freezing process, soil moisture reduces the hydraulic conductivity and leads to either more surface runoff due to decreasing infiltration or higher soil moisture content due to restricted drainage (Zhang and Armstrong 2001).

Since changes of soil thermal and hydraulic regimes have significant influences on earth systems, their variability is also affected by complex climatic and non-climatic factors. Variability in soil thermal and hydraulic regimes occurs through changes of soil temperature and moisture. Previous studies have largely paid attention to climate factors (Shiklomanov 2012), such as air temperature, precipitation, and snow depth. However, soil thermal and hydraulic regimes depend on multiple, complex

interactions among soil, vegetation, snow, and hydrology (Hinzman et al. 1997; Zhang et al. 1997; Park et al. 2013). Changes in these factors can influence heat and water exchange on the surface and in the soil and modulate the relationship between air and soil temperatures. Previous studies demonstrated that snow depth can be regarded as an important influencing factor to soil temperature, because of the insulating effect (Stieglitz et al. 2003; Zhang et al. 2005). In particular, snow accumulation, snow duration, timing, and quantity during the winter play significant roles in determining how air temperature signal propagates to the ground (Zhang 1996; Park et al. 2013). In fact, non-climate factors have important influences on soil thermal and hydraulic regimes, such as subsurface properties, vegetation cover, and types among others. Nevertheless, these non-climate factors are difficult to collect and quantify in the field.

The importance of studying the limits and difficulties in measuring soil thermal and hydraulic regimes is clear. Heihe River Basin, the second largest inland river basin in northwest China, has special hydro-ecosystem characteristics (“Study area” section). Changes to soil thermal and hydraulic regimes have had noticeable effects in local hydrological process and the ecological environment. To address this, the goals of this study are the following:

- (1) To assess climate change based on observational air temperature and precipitation dataset. This is intended to serve as evidence for a warming climate.
- (2) To evaluate soil thermal and hydraulic regimes during 1984–2013 in the Heihe River Basin. This is intended to provide the importance of implications for variability in soil temperature, moisture and frozen days (FD).
- (3) To explore the potential driving variables of FD, including climatic and non-climatic factors.

Material and methods

Study area

This research was carried out in the Heihe River Basin, the second largest inland river basin in northwest China (97° 42' E–102° 04' E and 37° 45'–42°

40° N, an area of ~ 128,000 km²) (Peng et al. 2016) (Fig. 1). The river flows northward through a piedmont diluvia-alluvial plain, an alluvial-lacustrine plain, and a desert. It also flows three different climate zones: a cold and humid (or semi-arid) mountain zone, a mid-stream temperate zone, and a downstream warm temperate zone (Peng et al. 2016). Generally, climate in the Heihe River Basin is dry, with infrequent but concentrated precipitation (annual precipitation ranges from 50 to 200 mm, but with strong evaporation, e.g., up to 3755 mm in the downstream zone), strong winds (mean annual wind speed is about 4.2 m/s and, on average, 54 days of fresh gale (34–40 knot winds) annually), strong solar radiation (the insolation duration is about 3000–4000 h in the mid-stream zone), and large temperature differences between day and night (Peng et al. 2016).

Combined with field investigations that include long-term soil temperature measured from drilled holes and physical detections using ground penetrating radar, the lower elevation limit of permafrost distribution in the Heihe River Basin is at about 3650 m a.s.l. Mean annual ground temperatures vary from around 0 to -1.5 °C, as the elevation increases. The areal extent of the permafrost region occupies approximately 14,100 km² or 10.3% of the Heihe River Basin (Wang et al. 2013a;

Fig. 2). The distribution of permafrost and SFG of the study area is used as the boundary of FD difference estimates in this study.

Air temperature and precipitation

Mean monthly air temperature (MMAT) and monthly precipitation data were collected from the China Meteorological Administration (CMA) from 12 meteorological stations in the Heihe River Basin (Fig. 1, Table 1). These data have quality-controlled station observations date from the 1950s and 1960s to 2013. Here, it focused on station records during the period 1980–2013 for this study. Data records are complete with the exception of some missing monthly data. It can be able to fill in missing data using linear regression based on highly correlated neighboring sites. Interpolated results were strongly correlated with observation data, as indicated by regression coefficients larger than 0.95.

Soil temperature

Daily soil temperature data are available for 12 sites in the Heihe River Basin (Fig. 1) from the CMA. These are measured at 0.00, 0.05, 0.1, 0.15, 0.2, 0.4, 0.5, 0.8, 1.6, and 3.2 m depths. The timeline of records vary among

Fig. 1 The location of the Heihe River Basin. The elevation varies from 600 to 5600 m. There are 12 meteorological stations from CMA in this study area

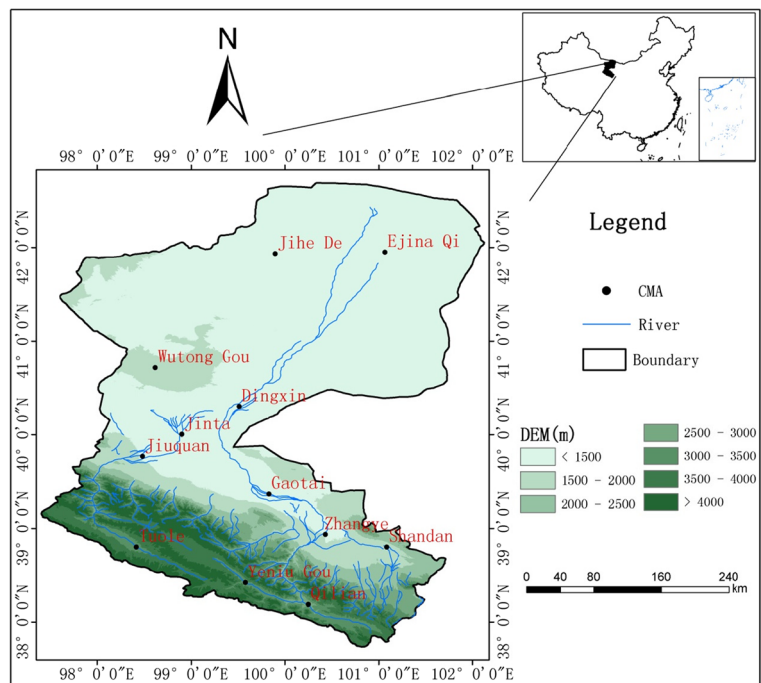
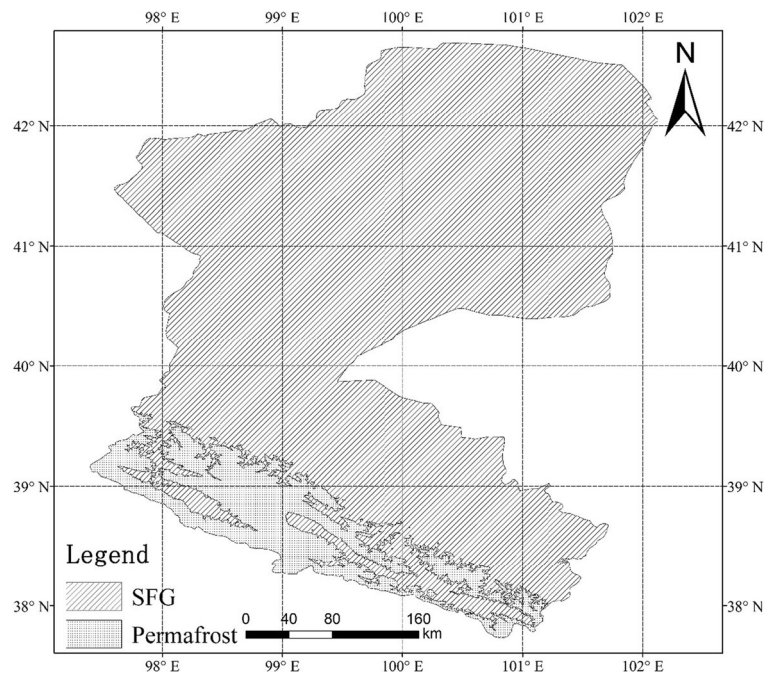


Fig. 2 Map of frozen ground distribution in Heihe River Basin

stations, with some observations dating back to the late 1950s and 1960s. Station records are available through 2006 (Wang et al. 2014).

Normalized difference vegetation index

The NDVI dataset used in this study was provided by Environmental and Ecological Science Data

Center for West China (<http://westdc.westgis.ac.cn/>). It is produced by the Global Inventory Modeling and Mapping Studies (GIMMS) team and is available for the period 1982–2006. It is derived from NOAA AVHRR data, available at 15-day intervals and an 8-km spatial resolution (Tourre et al. 2008). In this study, datasets for the period 1984–2006 are used.

Table 1 Geographical information for meteorological stations in the Heihe River Basin (China). The time is just the soil temperature time duration

Station ID	Station name	Longitude (°E)	Latitude (°N)	Elevation (m)	Time
52,267	Ejina Qi	101.07	41.95	940.5	1959–2006
52,343	Jihe De	99.90	41.93	965.6	1958–1986
52,441	Wutong Gou	98.62	40.72	1591.0	1965–1988
52,446	Dingxin	99.52	40.30	1177.4	1955–2006
52,447	Jinta	98.90	40.00	1270.5	1989–2006
52,533	Jiuquan	98.48	39.77	1477.2	1951–2006
52,546	Gaotai	99.83	39.37	1332.2	1952–2006
52,633	Tuole	98.42	38.80	3367.0	1956–2006
52,645	Yeniu Gou	99.58	38.42	3180.0	1959–2006
52,652	Zhangye	100.43	38.93	1482.7	1951–2006
52,657	Qilian	100.25	38.18	2787.4	1956–2006
52,661	Shandan	101.08	38.80	1764.6	1952–2006

Table 2 Model configuration used in this study

Contents	Description
Map projection	Lambert
Vertical layer	18 sigma
Turbulence	Holtslag PBL
Cumulus clouds	Grell with Frish-Chappell
Radiation	NCAR CCM3
Land surface processes	NCAR CLM3.5
Ocean surface fluxes	Zeng scheme
Lateral boundary	Relaxation (exponential)
Pressure gradient	Hydrostatic deduction
Simulation period	Jan 1982 to Dec 2013 (32 years)

Table 3 Multi-year mean seasonal and annual air temperature and precipitation in the Heihe River Basin

	Air temperature (°C)	Precipitation (mm)
Spring	7.54	26.05
Summer	19.60	104.15
Autumn	5.62	27.91
Winter	- 8.93	3.96
Year	5.97	162.08

Model

The International Centre for Theoretical Physics (ICTP) Regional Climate Model version 4 (RegCM4) was used in this study. The model includes multiple alternatives of land surface schemes, through a coupled Community Land Model (CLM 3.5), in addition to the original existing biosphere-atmosphere transfer scheme (BATS). CLM3.5 is a “third generation” land surface model, developed and supported by the National Center for Atmospheric Research (NCAR). It simulates complicated land physical processes, such as the land-atmosphere exchanges of energy, momentum, water, and carbon. CLM3.5 is considered as a more complex and advanced model than BATS for its finer vertical soil

and snow layer resolution, tiling structure, subsurface lateral runoff, and direct carbon calculation. Further details of both BATS and CLM3.5 schemes are presented in Steiner et al. (2009) and Wang et al. (2013b).

Model initial state and boundary condition data are from the National Centre for Environmental Prediction (NCEP) NCAR II reanalysis dataset. Lateral boundary conditions are provided every 6 h. Sea surface temperature (SST) data, collected at a 1° × 1° spatial resolution and 7-day temporal interval, are generated by the Integrated Global Ocean Service System and are spatially and temporally interpolated as the initial and boundary conditions of SST. 10' × 10' terrain data and United States Geological Survey (USGS) Global Land Cover Characterization (GLCC) data based on satellite observations are used as the topographic and vegetation inputs (Wang et al. 2013a, b). Table 2 shows the major parameterization schemes used in this experiment and demonstrate that

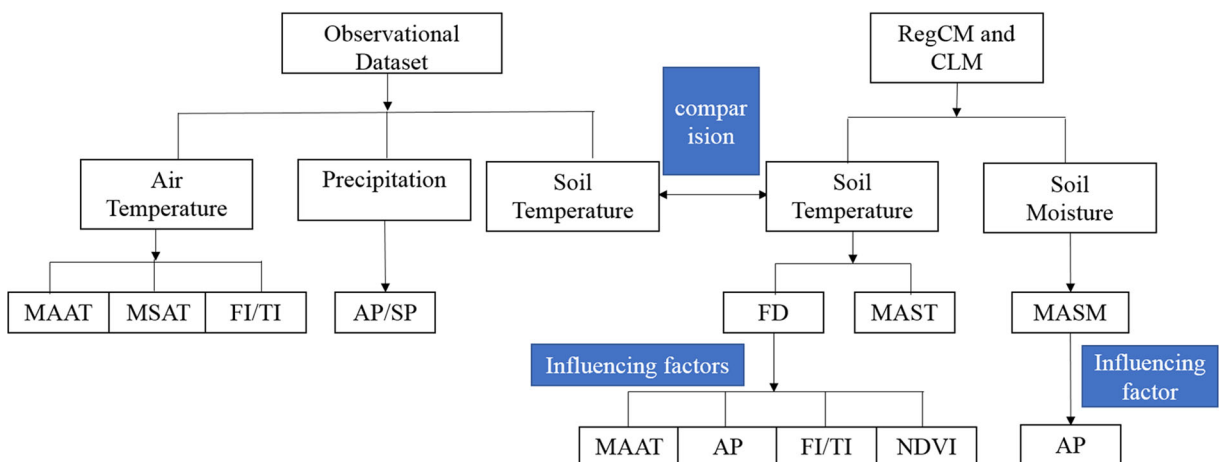


Fig. 3 The flow chart of the procedure of the data processing and application in this study. All the abbreviations can be seen in the article. The blue text boxes indicate the associations with each other

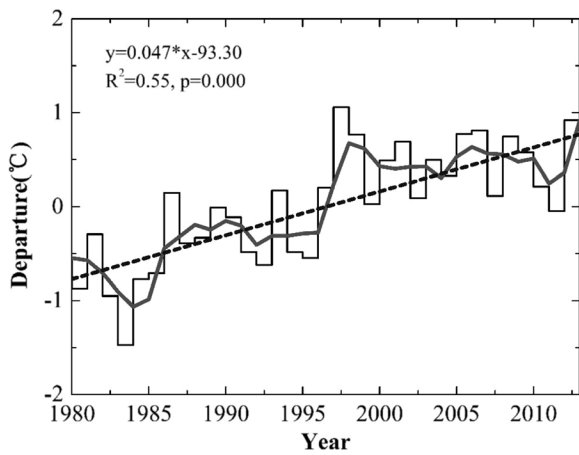


Fig. 4 Changes of mean annual air temperature during 1980–2013 in the Heihe River Basin. The solid black line is 3-year smoothing average, dash black line is the linear trend

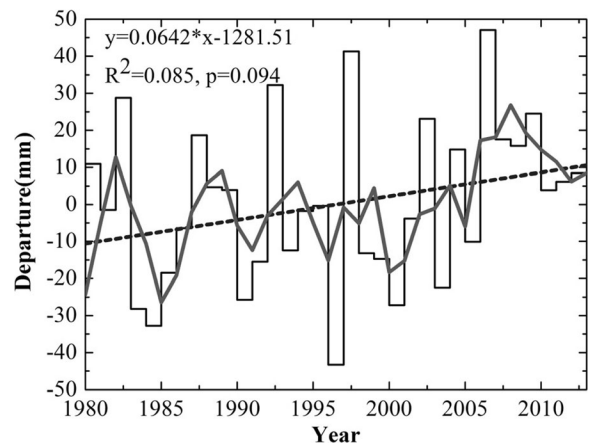


Fig. 6 Changes of annual precipitation during 1980–2013 in the Heihe River Basin. The solid bold black line is 3-year smoothing average, dash black line is the linear trend

these initialization parameters are suitable to this region (Wang et al. 2013a, b). The time period 1984–2013 was chosen in this study.

Methods

Air temperature and precipitation from 12 stations are used to compute the MAAT, mean seasonal air

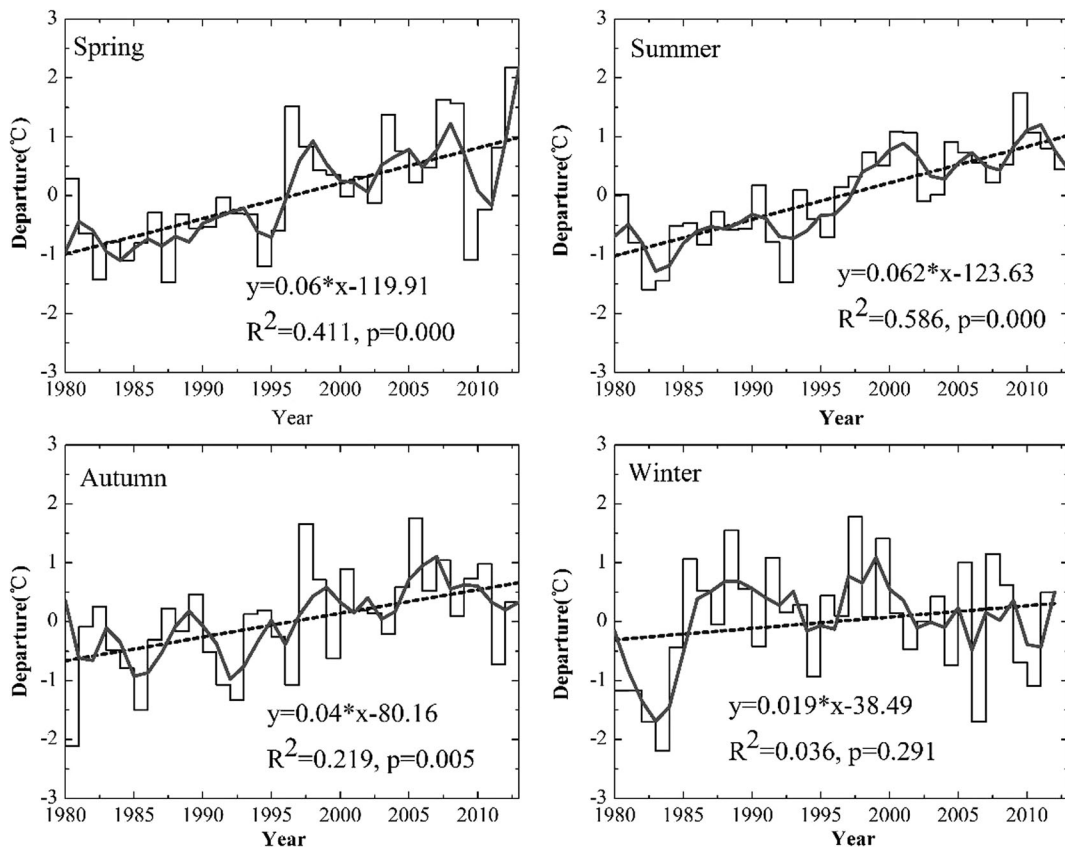


Fig. 5 Changes of mean seasonal air temperature in the Heihe River Basin. The solid black line is 3-year smoothing average, dash black line is the linear trend

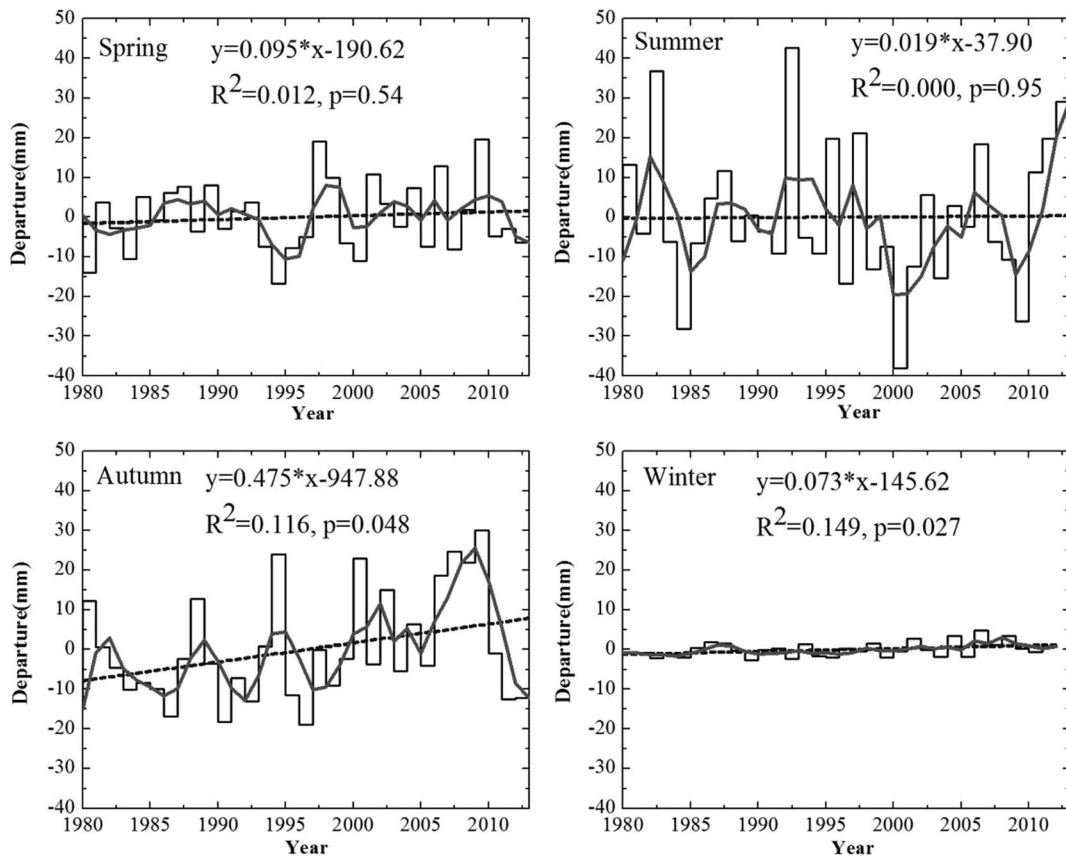


Fig. 7 Changes of seasonal precipitation during 1980–2013 in the Heihe River Basin. The solid bold black line is 3-year smoothing average, dash black line is the linear trend

temperature (MSAT), annual precipitation (AP), and seasonal precipitation (SP). Linear regression is used to analyze temperature and precipitation trends.

Table 4 Comparison between simulated and observational soil temperature at different soil depth

Depth (cm)	Fitted equation	R^2	p	Bias ($^{\circ}\text{C}$)
5	$y = 0.88*x - 0.39$	0.94	0.00	-1.41
10	$y = 0.98*x - 1.33$	0.95	0.00	-1.46
15	$y = 1.03*x - 1.81$	0.96	0.00	-1.49
20	$y = 1.07*x - 2.09$	0.96	0.00	-1.43
40	$y = 1.03*x - 1.73$	0.96	0.00	-1.40
50	$y = 1.04*x - 1.48$	0.97	0.00	-1.02
80	$y = 1.20*x - 3.15$	0.97	0.00	-0.91
160	$y = 1.42*x - 5.50$	0.96	0.00	-0.85

y is the simulated soil temperature, and x is the observational soil temperature

Annual air freezing (thawing) index is the sum of temperature for all days with temperatures below (above) 0°C during the freezing (thawing) period. The annual freezing period was defined as 1 July through 30 June of the following year. The annual thawing period was defined as 1 January through 31 December (Peng et al. 2016). Air temperature datasets are used to compute the freezing and thawing indices.

In order to evaluate the simulated soil temperature and moisture at different soil depths based on observational soil temperature, the model first linearly interpolated the 12 soil depth measures (0.05, 0.1, 0.15, 0.2, 0.3, 0.4, 0.5, 0.6, 0.8, 1.2, 1.6, and 2.8 m.). Second, it extracted the soil temperature values corresponding to the stations' latitude and longitude coordinates. Third, it used linear correlation with adjusted R^2 , p value, and bias variables to evaluate results. In addition, soil temperature and moisture anomalies from the 12 sites were

calculated during 1984–2013, and its variability analyzed by linear correlation.

Frozen days defined the number of days in which soil temperature was below 0 °C in 1 year. In this study, area-averaged FD at each depth in SFG and permafrost regions are used to determine changes.

In this study, linear regression and correlation analysis are not only used to analyze climate change trends, evaluate the simulated results, and determine FD trends, but also explore the potential driving variables in freeze days, soil temperature, and soil moisture. The results were tested for statistical significance.

In order to illustrate the procedure of the data processing and application in this study, a flow chart is inserted here (Fig. 3).

Results

Climate changes

The multi-year averaged MAAT from the 12 stations in the Heihe River Basin was 5.97 °C (Table 3). The warmest was 19.6 °C during summer, followed by 7.54 °C in spring, then 5.62 °C in autumn, and the coldest in winter at − 8.93 °C during 1980–2013. MAAT increased at a rate of 0.47 °C/decade during 1980–2013 (Fig. 4). In addition to this overall long-term increase, the MAAT time series also indicates some interesting patterns of inter-decadal variability, including periods of slight negative change. MAAT appears to have decreased until 1984, followed by a

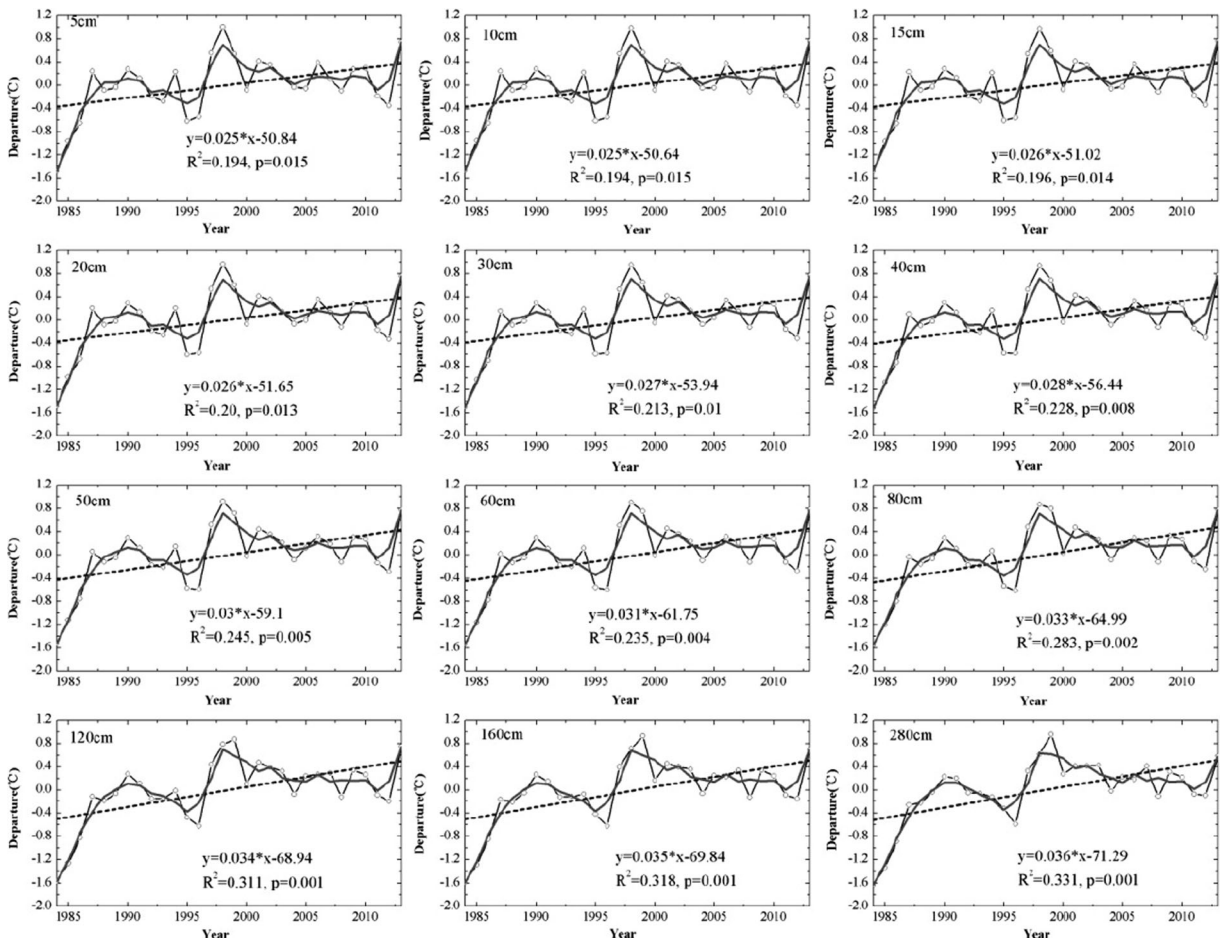


Fig. 8 Changes of mean annual soil temperature at different soil depth in the Heihe River Basin. The solid bold black line is 3-year smoothing average, dash black line is the linear trend

sharp increase until 1998, and by a small decrease until 2012. The overall 1980–2013 change is therefore largely driven by the increase during the 1984–1998 period. MSAT changes show that the most rapid increase is 0.62 °C/decade in summer, followed by 0.6 °C/decade in spring, next 0.4 °C/decade in autumn, and finally a non-significant rate in winter during 1980–2013 (Fig. 5).

The multi-year average annual precipitation was approximately 162 mm (Fig. 6). There is distinct seasonality in precipitation, falling mainly in summer (104 mm) and less in other seasons (Fig. 7, Table 3). There is no trend in AP with large annual variation. Similarly, although rainfall also occurs in spring and

summer, there is only a small increasing trend in autumn and winter with p value < 0.05 (Fig. 7).

Soil temperature changes

Results of the evaluation of soil temperature derived from model simulations indicated that the simulated soil temperature in samples deeper than 15 cm was overestimated. At depths shallower than 15 cm, it was underestimated (Table 4). The soil temperature bias is -0.91 and -0.85 °C at 80 and 160 cm, respectively, and less than -1 °C at soil depths shallower than 80 cm. The correlation coefficient R^2 is larger than 0.94. The simulation does reflect soil temperature trend efficiently.

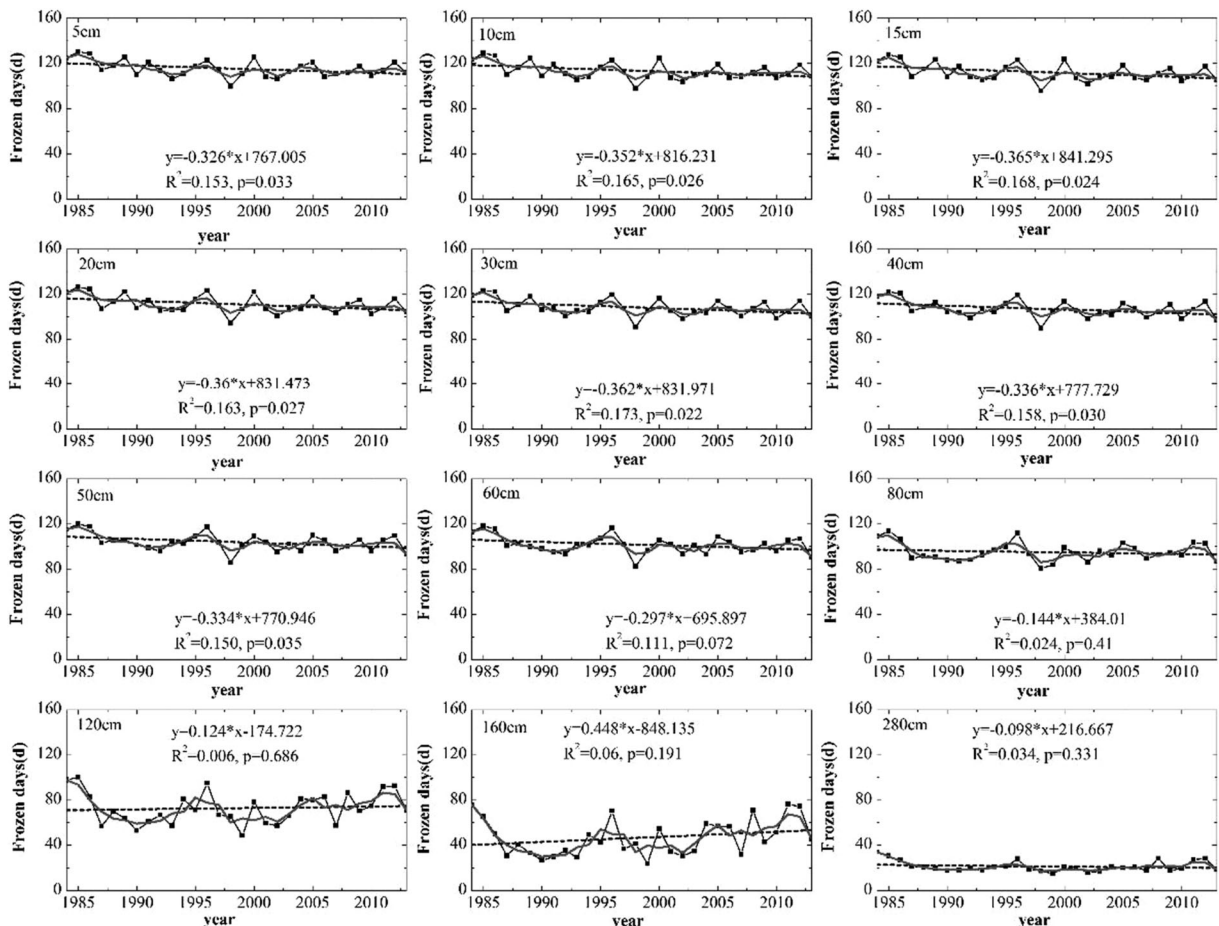


Fig. 9 Changes of annual freeze days in seasonally frozen ground at different depth in the Heihe River Basin. The solid black line is 3-year smoothing average, dash black line is the linear trend

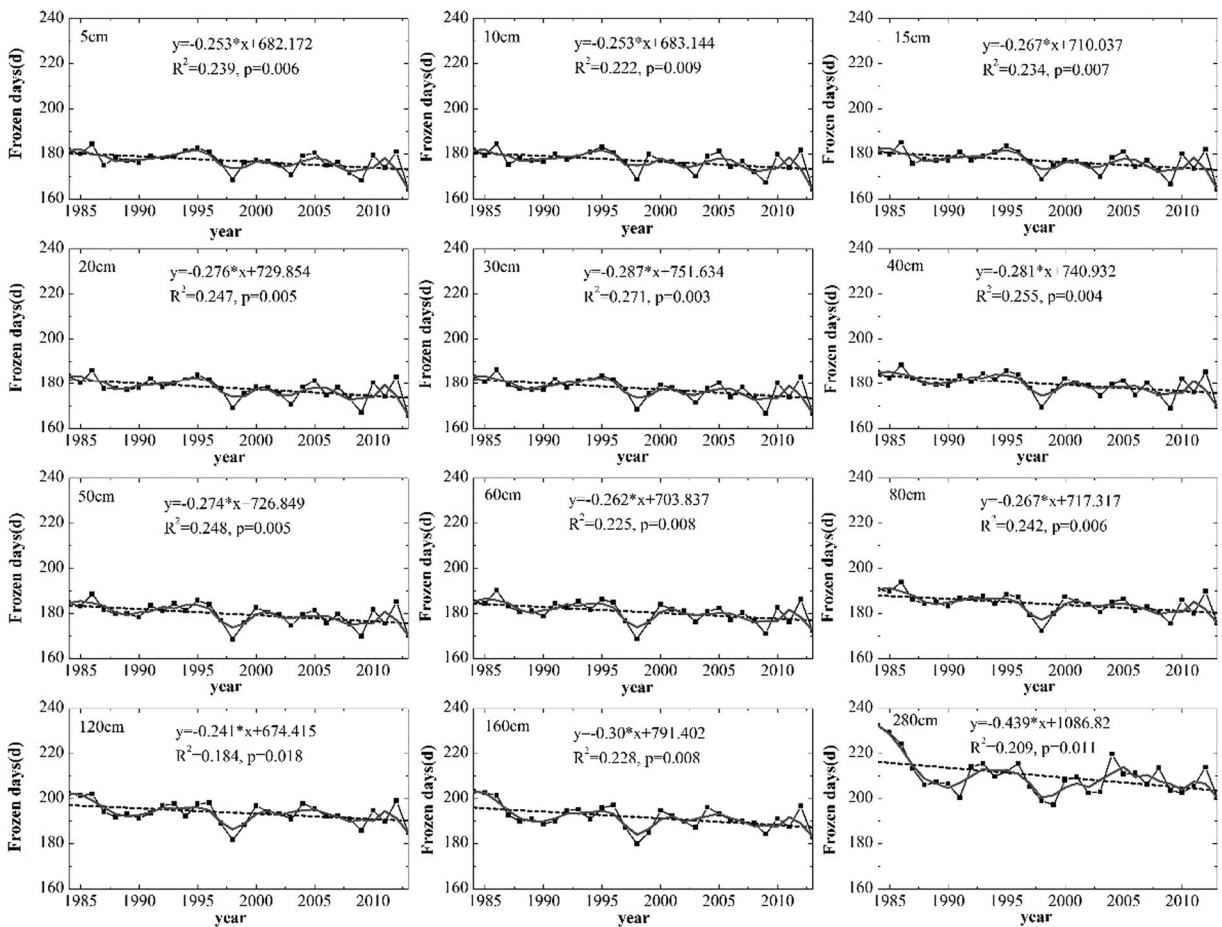


Fig. 10 Changes of annual freeze days in permafrost at different depth in the Heihe River Basin. The solid black line is 3-year smoothing average, dash black line is the linear trend

Therefore, soil temperature derived from model can serve as the soil freeze/thaw process in this study.

Area-averaged soil temperature increased significantly at each depth during 1984–2013 (Fig. 8). The fastest increase rate was 0.36 °C/decade at 280 cm, and the slowest increase was 0.25 °C/decade at 5 cm. The rate of soil temperature increase is higher at deeper soil depths, with an average net change of about 0.9 °C. In addition to this overall long-term increase, the time series also indicates some interesting patterns of inter-decadal variability, including periods of slight negative changes. Taking the mean annual soil temperature (MAST) at a depth of 20 cm as an example, it appears to increased sharply until 1990, followed by a decrease until 1995, and the next followed by a slight decrease until 2012. The overall 1984–2013 change is therefore largely

driven by the increase during the 1984–1990 period. Time series of soil temperature at other depths is also similar in character.

Frozen days

The time series of area-averaged FD in SFG shows a statistically significant decreasing trend at each depth during 1984–2013, except at 50 cm (Fig. 9). The trend decreased between -3.26 and -3.65 day/decade, with a net change of about 9.7 and 11 days during that time. At depths less than 50 cm, multi-year averaged FD was between 103 and 115 days.

In permafrost regions, FD also had a declining trend (p value < 0.05 ; Fig. 10). The multi-year average FD was between 176 and 210 days. This

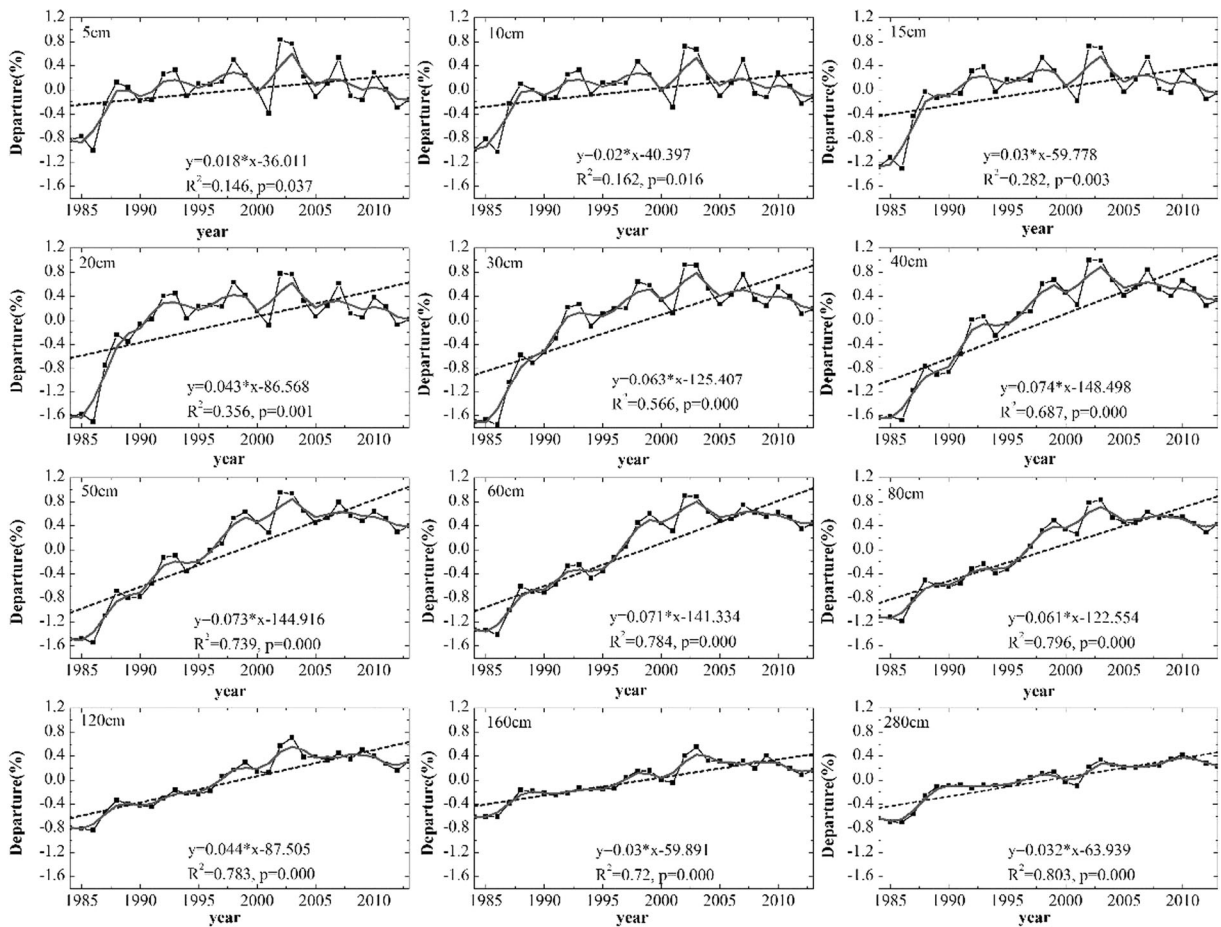


Fig. 11 Changes of mean annual soil moisture at different depth in the Heihe River Basin. The solid black line is 3-year smoothing average, dash black line is the linear trend

decreasing rate ranged between -2.4 and -4.3 day/decade, demonstrating a net change of between 7 and 13 days in permafrost regions during the years 1984–2013.

Soil moisture

It is found a significantly increasing trend of soil moisture at each soil depth during the years 1984–2013, ranging from 0.018 to 0.074% per year (Fig. 11). Soil moisture variation is similar in each depth. Here, taking the soil moisture at 20 cm as an example, the overall long-term increasing trend shows some interesting internal decade variability in the time series. There was a sharp increase until

1993, followed by a slight increase until 2003, and followed by a slight decrease until 2013.

Discussion

Comparison with previous results

In this study, we noted rising temperature, but without a significantly increasing trend in precipitation, during 1980–2013. These results are roughly consistent with previous results (Lan et al. 2015). The multi-model ensemble mean of Coupled Model Inter-comparison Project phase 5 (CMIP5) models indicate an increase of 0.17 °C/decade from 1901 to 2005 in an arid area

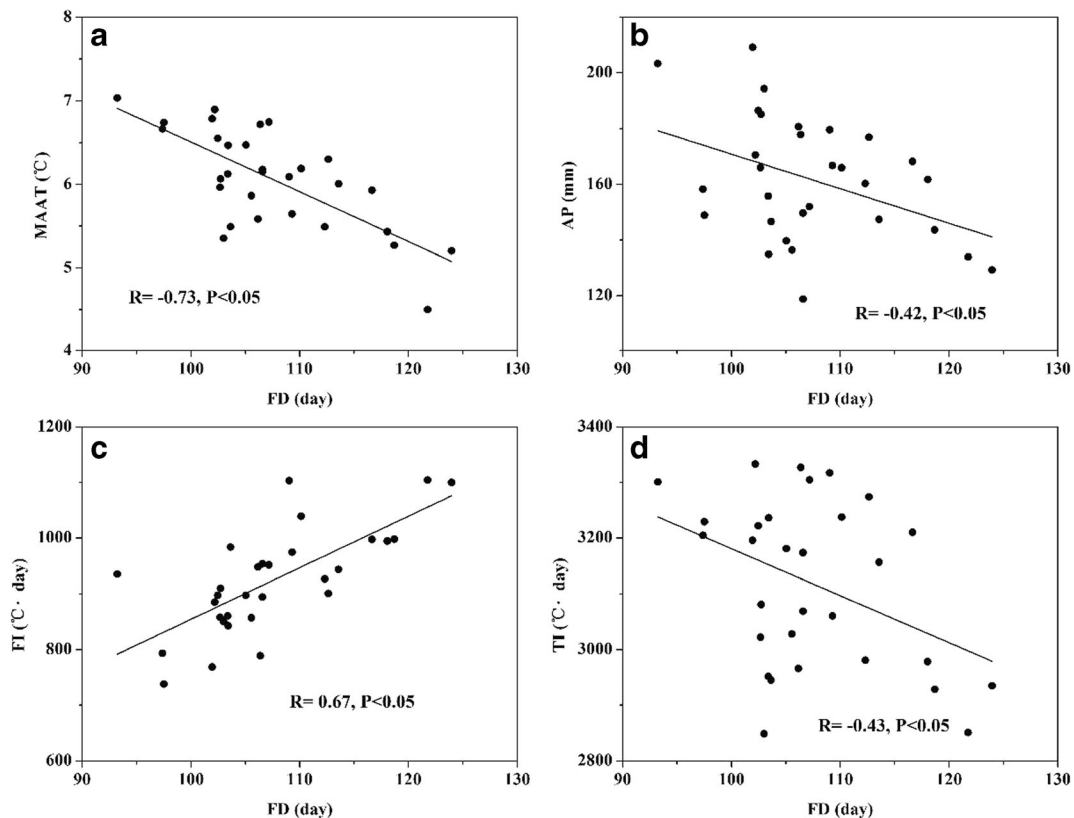


Fig. 12 Correlation between freeze days and MAAT (a), AP (b), FI (c), and TI (d) in the Heihe River Basin

(Zhao et al. 2014), and 0.2–0.3 °C/decade from 1951 to 2005 in central Asia (Jiang et al. 2013).

Influencing factors of freeze day

The trend of FD decreased significantly during the years 1984–2013 everywhere in SFG or permafrost regions over the Heihe River Basin. To determine what may drive potential changes in FD, MAAT, freezing index, thawing index, and AP were analyzed (Fig. 12). MAAT was significantly correlated with the FD time series at $R = -0.73$, indicating that 53% of the variance in FD can be accounted for by MAAT changes. This negative correlation illustrated that, as temperatures increased from 1984 to 2013, FD decreased. The correlation between FI, TI, and FD was statistically significant and strong ($R = 0.67$ and $R = -0.43$, respectively), indicating that 45 and 19% of FD variability can be accounted for. The correlation coefficient between AP and FD was -0.42 , indicating a weak negative association

comparing to MAAT. Greater AP corresponded to a lower FD. Furthermore, MAAT, AP, and TI are negatively correlated with FD for some reasons. MAAT is a variable reflecting solar radiation, which is the ground heat resource. Similarly, FI and TI are factors that accumulate air temperature. Precipitation changes may influence heat transfer through effects to soil moisture and thermal conductivity (Frauenfeld and Zhang 2011).

In addition of these climate factors, FD is also affected by other non-climatic factors (e.g., subsurface properties, soil moisture, snow depth, vegetation cover; Shiklomanov 2012). It found a negative correlation between NDVI and FD (Fig. 13). Mean annual NDVI was significantly correlated with the FD time series at $R = -0.69$, indicating that 48% of the variance in FD can be accounted for by changes in mean annual NDVI. Although the mean seasonal NDVI was negatively correlated with FD, the correlation was not as strong as mean annual NDVI. The negative correlation illustrated that, as

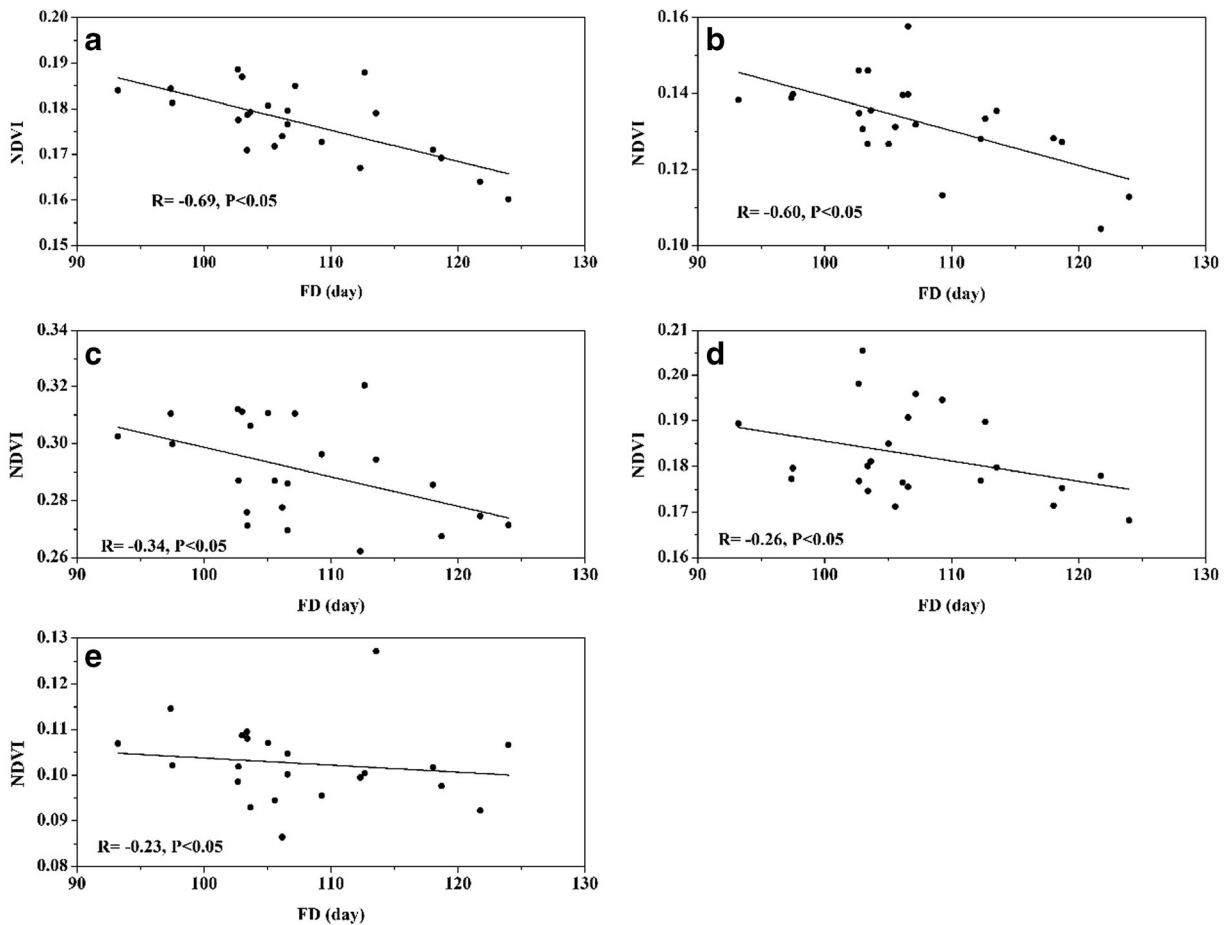


Fig. 13 Relationship between mean annual freeze days and NDVI in the Heihe River Basin. **a** Annual, **b** spring, **c** summer, **d** autumn, and **e** winter

NDVI increased, FD decreased. In winter, good vegetation cover can, like the snow, play a role in thermal insulation. While in summer, the vegetation can reflect more solar radiation and absorb less solar radiation that can reduce evaporation.

Relationship between temperature, precipitation, and soil temperature and moisture

It found a statistically significant increasing trend between MAST and mean annual soil moisture (MASM) at each soil depth during 1984–2013 over the Heihe River Basin (Figs. 8 and 11). To explore possible driving factors, the correlation between MAAT, AP and MAST, and MASM were analyzed. Taking soil depth at 20 cm as an example, MAAT was strongly and positively correlated with MAST and

soil moisture, with $R = 0.88$, and $R = 0.63$, indicating that 77 and 40% of the variance in soil temperature and soil moisture can be accounted for by their change, respectively. AP correlated with soil moisture at $R = 0.47$, indicating 22% of the variance in soil moisture can be accounted for by its changes. Soil freeze and thaw process are followed by heat changes. The soil freezing process would release latent heat by water-ice phase changes, thus lessening the soil cooling trend. The soil thawing process would absorb heat to lessen the soil warming trend. When the soil is transitioning from a thawed to a frozen state, its thermal conduction would be higher and thermal capacity would be lower that would affect the surface heat exchanges (Zhao et al. 2004; Subin et al. 2013). Thus, climate changes are strongly associated with soil thermal and hydraulic regimes.

Conclusions

This study investigated changes of soil thermal and hydraulic regimes, and their association with climate change over the Heihe River Basin. Here, we summarize the main findings.

Rising air temperature was noted from the 12 stations' air temperature and precipitation records. MAAT had an increasing trend at 0.47 °C/decade, and MSAT rose the fastest at 0.62 °C/decade. Precipitation did not increase significantly but rather showed large amplitudes and frequent fluctuations.

Soil temperature and moisture at each depth both showed increasing trends. Soil temperature increased at a rate ranging between 0.25 and 0.36 °C/decade, with a net change of about 0.9 °C during the years 1984–2013. Soil moisture increased at rate ranging from 0.018 to 0.074%/year. Soil temperature is most strongly correlated with air temperature, while soil moisture is strongly associated with precipitation.

Frozen days was an important factor demonstrating the soil freeze/thaw process in this cold region. Area-averaged FD ranged between 21.4 and 115.4 days in SFG, and between 176.8 and 210 days in the permafrost region. A pronounced decreasing trend of FD was found during the years 1984–2013 in the Heihe River Basin. FD is most strongly related with air temperature. In addition, NDVI, freezing/thawing index, and precipitation, are also significantly correlated to FD.

Acknowledgments This study was funded by the National Natural Science Foundation of China (Grant No. 91325202, 41601063), the National Key Scientific Research Program of China (Grant No. 2013CBA01802), and the Fundamental Research Funds for the Central Universities (lzujbky-2015-217). We appreciate the thoughtful input from two anonymous reviewers, whose comments improved this manuscript. The land cover data was obtained from the Environmental and Ecological Science Data Center for West China (<http://westdc.westgis.ac.cn/>). We acknowledge computing resources and time at the Supercomputing Center of Cold and Arid Region Environment and Engineering Research Institute of Chinese Academy of Sciences.

References

- Chang, C., & Hao, X. (2001). Source of N₂O emission from a soil during freezing and thawing. *Phyton*, *41*, 49–60.
- Chen, Y., Tessier, S., Mackenzie, A. F., & Laverdiere, M. R. (1995). Nitrous oxide emission from an agricultural soil subjected to different freeze-thaw cycles. *Agriculture Ecosystems & Environment*, *55*, 123–128.
- Deluca, T. H., Keeney, D. R., & Mccarty, G. W. (1992). Effect of freeze-thaw events on mineralization of soil nitrogen. *Biology and Fertility of Soils*, *14*, 116–120.
- Ford, T. W., & Frauenfeld, O. W. (2016). Surface-atmosphere moisture interactions in the frozen ground regions of Eurasia. *Scientific Reports*, *6*, 19163.
- Frauenfeld, O. W., & Zhang, T. (2011). An observational 71-year history of seasonally frozen ground changes in the Eurasian high latitudes. *Environmental Research Letters*, *6*(8), 44024–44031.
- Gruber, S., Hoelzle, M., & Haeblerli, W. (2004). Permafrost thaw and destabilization of alpine rock walls in the hot summer of 2003. *Geophysical Research Letters*, *31*(13), 405–407.
- Guo, D., & Wang, H. (2016). CMIP5 permafrost degradation projection: a comparison among different regions. *Journal of Geophysical Research: Atmospheres*, *121*, 4499–4517.
- Harris, M. M., & Safford, O. L. (1996). Effects of season and four tree species on soluble carbon content in fresh and decomposing litter of temperate forests. *Soil Science*, *161*, 130–135.
- Henry, H. A. L. (2008). Climate change and soil freezing dynamics: historical trends and projected changes. *Climatic Change*, *87*, 421–434.
- Hinzman, L. D., Kane, D. L., Gieck, R. E., & Everett, K. R. (1991). Hydrologic and thermal properties of the active layer in the Alaskan Arctic. *Cold Regions Science & Technology*, *19*, 95–110.
- Hinzman, L. D., D. J. Goering, T. C. Kinney & S. Li. (1997). Numeric simulation of thermokarst formation during disturbance. *Disturbance and Recovery in Arctic Lands*.
- Hinzman, L. D., Bettez, N. D., Bolton, W. R., Chapin, F. S., Dyrgerov, M. B., Fastie, C. L., et al. (2005). Evidence and implications of recent climate change in northern Alaska and other arctic regions. *Climatic Change*, *72*, 251–298.
- Intergovernmental Panel on Climate Change (IPCC) (2013). Climate Change 2013: The physical science basis, in the Fifth Assessment Report of the Intergovernmental Panel on Climate Change. In: T. F. Stocker et al. (Eds.), (pp. 161–162), Cambridge: Cambridge University Press.
- Jeong, J. H., Kug, J. S., Kim, B. M., Min, S. K., Linderholm, H. W., Ho, C. H., et al. (2012). Greening in the circumpolar high-latitude may amplify warming in the growing season. *Climate Dynamics*, *38*, 1421–1431.
- Jiang, Y., Wu, H., Bureau, L. M., & Lishui. (2013). Simulation capabilities of 20 CMIP5 models for annual mean air temperatures in Central Asia. *Progressus Inquisitiones De Mutatione Climatis*, *9*, 110–116.
- Kane, D. L., Hinzman, L. D., & Zurling, J. P. (1991). Thermal response of the active layer to climatic warming in a permafrost environment. *Cold Regions Science & Technology*, *19*, 111–122.
- Kaverin, D., G. Mazhitova, A. Pastukhov, and F. Rivkin (2012). The transition layer in permafrost-affected soils, Northeast European Russia. *Proc. 10th Int. Conf. on Permafrost*, 145–148.
- Koven, C. D., Riley, W. J., & Stern, A. (2013). Analysis of permafrost thermal dynamics and response to climate change in the CMIP5 earth system models. *Journal of Climate*, *26*, 1877–1900.

- Lan, Y. C., Ding, H. W., Hu, X. L., Shi, M. X., & Ma, Q. (2015). The seasonal change characteristics of temperature, precipitation in the mountain areas of the Heihe River and their regional differences. *Mountain Research*, 33, 294–302.
- Larsen, K. S., Jonasson, S., & Michelsen, A. (2002). Repeated freeze–thaw cycles and their effects on biological processes in two arctic ecosystem types. *Applied Soil Ecology*, 21, 187–195.
- Luo, D., Wu, Q., Jin, H., Marchenko, S. S., Lü, L., & Gao, S. (2016). Recent changes in the active layer thickness across the Northern Hemisphere. *Environmental Earth Sciences*, 75, 1–15.
- Melick, D. R., & Seppelt, R. D. (1992). Loss of soluble carbohydrates and changes in freezing point of Antarctic bryophytes after leaching and repeated freeze–thaw cycle. *Antarctic Science*, 4, 399–404.
- Mu, C., Zhang, T., Wu, Q., Peng, X., Cao, B., Zhang, X., Cao, B., & Cheng, G. (2015). Editorial: organic carbon pools in permafrost regions on the Qinghai–Xizang (Tibetan) Plateau. *The Cryosphere*, 9, 479–486.
- Muller, C., Martin, M., Stevens, R. J., Laughlin, R. J., Kammann, C., Jcg, O., & Jager, H. J. (2002). Processes leading to N₂O emissions in grassland soil during freezing and thawing. *Soil Biology & Biochemistry*, 34, 1325–1331.
- Oztaş, T., & Fayetorbay, F. (2003). Effect of freezing and thawing processes on soil aggregate stability. *Catena*, 52, 1–8.
- Park, H., Walsh, J., Fedorov, A. N., & Sherstiukov, A. B. (2013). The influence of climate and hydrological variables on opposite anomaly in active layer thickness between Eurasian and North American watersheds. *Cryosphere Discussions*, 7, 631–645.
- Park, H., Kim, Y., & Kimball, J. S. (2016). Widespread permafrost vulnerability and soil active layer increases over the high northern latitudes inferred from satellite remote sensing and process model assessments. *Remote Sensing of Environment*, 175, 349–358.
- Peng, X. Q., Zhang, T. J., Cao, B., Wang, Q. F., Wang, K., Shao, W. W., & Guo, H. (2016). Changes in freezing–thawing index and soil freeze depth over the Heihe River Basin, Western China. *Arctic Antarctic & Alpine Research*, 48, 161–176.
- Pepin, N., Bradley, R., Diaz, H. F., Baraer, M., Caceres, E. B., Forsythe, N., Fowler, H., Greenwood, G., Hashmi, M. Z., Liu, X. D., Miller, J. R., Ning, L., Ohmura, A., Palazzi, E., Rangwala, I., Schoner, W., Severskiy, I., Shahgedanova, M., Wang, M. B., Williamson, S. N., & Yang, D. Q. (2015). Elevation-dependent warming in mountain regions of the world. *Nature Climate Change*, 5, 424–430.
- Schädel, C., Bader, M. K. F., Schuur, E. A. G., Biasi, C., Bracho, R., Čapek, P., Baets, S. D., Diáková, K., Ernakovich, J., & Estoparagones, C. (2016). Potential carbon emissions dominated by carbon dioxide from thawed permafrost soils. *Nature Climate Change*, 6, 950–953.
- Schuur, E. A. G., McGuire, A. D., Schädel, C., Grosse, G., Harden, J. W., Hayes, D. J., Hugelius, G., Koven, C. D., Kuhry, P., & Lawrence, D. M. (2015). Climate change and the permafrost carbon feedback. *Nature*, 2015, 171–179.
- Screen, J. A., & Simmonds, I. (2010). The central role of diminishing sea ice in recent Arctic temperature amplification. *Nature*, 464, 1334–1337.
- Serreze, M. C., Walsh, J. E., Iii, F. S. C., Osterkamp, T., Dyrgerov, M., Romanovsky, V., et al. (2000). Observational evidence of recent change in the northern high-latitude environment. *Climatic Change*, 46, 159–207.
- Shiklomanov, N. I. (2012) Non-climatic factors and long-term, continental-scale changes in seasonally frozen ground. *Environmental Research Letters*, 7.
- Six, J., Bossuyt, H., Degryze, S., & Deneff, K. (2004). A history of research on the link between (micro) aggregates, soil biota, and soil organic matter dynamics ☆. *Soil & Tillage Research*, 79, 7–31.
- Skogland, T., Lomeland, S., & Goksøyr, J. (1988). Respiratory burst after freezing and thawing of soil: experiments with soil bacteria. *Soil Biology & Biochemistry*, 20, 851–856.
- Slater, A. G., & Lawrence, D. M. (2013). Diagnosing present and future permafrost from climate models. *Journal of Climate*, 26, 5608–5623.
- Steiner, A. L., Pal, J. S., Rauscher, S. A., Bell, J. L., Diffenbaugh, N. S., Boone, A., Sloan, L. C., & Giorgi, F. (2009). Land surface coupling in regional climate simulations of the West African monsoon. *Climate Dynamics*, 33, 869–892.
- Stieglitz, M., Déry, S. J., Romanovsky, V. E., & Osterkamp, T. E. (2003). The role of snow cover in the warming of arctic permafrost. *Geophysical Research Letters*, 30, 54–51.
- Subin, Z. M., Koven, C. D., Riley, W. J., Torn, M. S., Lawrence, D. M., & Swenson, S. C. (2013). Effects of soil moisture on the responses of soil temperatures to climate change in cold regions. *Journal of Climate*, 26, 3139–3158.
- Tourre, Y. M., Jarlan, L., Lacaux, J. P., Rotela, C. H., & Lafaye, M. (2008). Spatio-temporal variability of NDVI–precipitation over southernmost South America: possible linkages between climate signals and epidemics. *Environmental Research Letters*, 3, 52–55.
- Vaz, R., Edwards, A. C., Shand, C. A., & Cresser, M. S. (1994). Changes in the chemistry of soil solution and acetic-acid extractable P following different types of freeze/thaw episodes. *European Journal of Soil Science*, 45, 353–359.
- Wang, F. L., & Bettany, J. R. (1993). Influence of freeze–thaw and flooding on the loss of soluble organic carbon and carbon dioxide from soil. *Journal of Environmental Quality*, 22, 709–714.
- Wang, Q. F., Zhang, T. J., Wu, J. C., Peng, X. Q., Zhong, X. Y., Mu, C. C., Wang, K., Wu, Q. B., & Cheng, G. D. (2013a). Permafrost characteristics over the Heihe River Basin in western China. *Journal of Food Agriculture & Environment*, 11, 1084–1085.
- Wang, X., Yang, M., Wan, G., Chen, X., & Pang, G. (2013b). Qinghai–Xizang (Tibetan) Plateau climate simulation using the regional climate model RegCM3. *Climate Research*, 57, 173–186.
- Wang, K., Zhang, T., & Zhong, X. (2014). Changes in the timing and duration of the near-surface soil freeze/thaw status from 1956 to 2006 across China. *The Cryosphere*, 9, 1321–1331.
- Wu, Q., Zhang, Z., Gao, S., & Ma, W. (2016). Thermal impacts of engineering activities and vegetation layer on permafrost in different alpine ecosystems of the Qinghai–Tibet Plateau, China. *The Cryosphere*, 10, 1695–1706.
- Yanai, Y., Toyota, K., & Okazaki, M. (2004). Effects of successive soil freeze–thaw cycles on soil microbial biomass and organic matter decomposition potential of soils. *Soil Science and Plant Nutrition*, 50, 821–829.
- Yi, S., Zhou, Z., Ren, S., Xu, M., Qin, Y., Chen, S., et al. (2011). Effects of permafrost degradation on alpine grassland in a

- semi-arid basin on the qinghai-tibetan plateau. *Environmental Research Letters*, 6(4), 45403–45409.
- Zhang, T. (1996). Some characteristics of the climate in northern Alaska, U.S.A. *Arctic & Alpine Research*, 28, 509–518.
- Zhang, T., & Armstrong, R. L. (2001). Soil freeze/thaw cycles over snow-free land detected by passive microwave remote sensing. *Geophysical Research Letters*, 28, 763–766.
- Zhang, T., Osterkamp, T. E., & Stamnes, K. (1997). Effects of climate on the active layer and permafrost on the north slope of Alaska, U.S.A. *Permafrost and Periglacial Processes*, 8, 45–67.
- Zhang, Y., W. Chen, S. L. Smith, D. W. Riseborough & J. Cihlar (2005) Soil temperature in Canada during the twentieth century: complex responses to atmospheric climate change. *Journal of Geophysical Research*, 110.
- Zhao, L., Ping, C. L., Yang, D., Cheng, G., Ding, Y., & Liu, S. (2004). Changes of climate and seasonally frozen ground over the past 30 years in Qinghai–Xizang (Tibetan) Plateau, China. *Global & Planetary Change*, 43, 19–31.
- Zhao, L., Wu, Q., Marchenko, S., & Sharkhuu, N. (2010). Thermal state of permafrost and active layer in Central Asia during the International Polar Year. *Permafrost and Periglacial Processes*, 21, 198–207.
- Zhao, T. B., Chen, L., & Ma, Z. G. (2014). Simulation of historical and projected climate change in arid and semiarid areas by CMIP5 models. *Science Bulletin*, 59, 412–429.